Examination of reductions in detected skylight background signal attainable in elastic backscatter lidar systems using polarization selection

S. A. Ahmed, Y. Hassebo, B. Gross, M. Oo, F. Moshary

Optical Remote Sensing Laboratory - The City College of the City University of New York
Convent Ave. & 140 St., New York, NY 10031, USA
E-mail: ahmed@ccny.cuny.edu

Abstract

Detected sky background light is an important limiting factor for daylight operation of lidar systems operating in the visible spectrum. We examine the efficacy and potential of a polarization selection technique, recently devised by us, which takes advantage of naturally occurring polarization properties of scattered sky light to minimize the detected sky background signal and which can be used in conjunction with linearly polarized elastic backscatter lidars. In this approach, a polarization selective lidar receiver is aligned to minimize detected skylight, while the polarization of the transmitted lidar signal is rotated to maintain maximum lidar backscatter signal throughput to the receiver detector, consequently maximizing detected signal to noise ratio. Results presented include lidar elastic backscatter measurements, at 532 nm which show as much as a factor of $\sqrt{10}$ improvement in signal-to-noise ratio over conventional un-polarized schemes. For vertically pointing lidars, the largest improvements are limited to symmetric early morning and late afternoon hours. For non-vertical scanning lidars, significant improvements are achievable over much more extended time periods, depending on the specific angle between the lidar and solar axes. A theoretical model that simulates the background skylight within the single scattering approximation showed good agreement with measured SNR improvement factors. Diurnally asymmetric improvement factors, sometimes observed, are explained by measured increases in PWV and subsequent modification of aerosol optical depth by dehydration from morning to afternoon. Finally, since the polarization axis follows the solar azimuth angle even for high aerosol loading, as demonstrated using radiative transfer simulations, it is possible to conceive automation of the technique.

1. Introduction

Polarization selective lidar systems have been used primarily for separating and analyzing polarization of lidar returns, for a variety of purposes, including examination of multiple scattering effects and for differentiating between different atmospheric scatterers and aerosols.[1-3] In the approach described here, the polarized nature of the sky background light is used to devise a polarization selective scheme to reduce the sky background power detected by a lidar receiver, leading to improved signal-to-noise ratios and attainable lidar sensitivities and effective ranges in daylight operation[4]. The technique is based on the fact that most of the energy in linearly polarized elastically backscattered lidar signals retains the transmitted polarization[1-3], while the received sky background power (P_b) observed by the lidar receiver shows polarization characteristics that depend on both the angle between the direction of the lidar and the direct sunlight, as well as the orientation of the detector polarization to the scattering plane. In particular, the sky background signal is minimized in the plane perpendicular to the scattering plane, while the difference between the in-plane component and the perpendicular components (i.e degree of polarization) depends solely on the scattering angle.

For a vertically pointing lidar, the scattering angle is simply the solar zenith angle (see Figure 1).

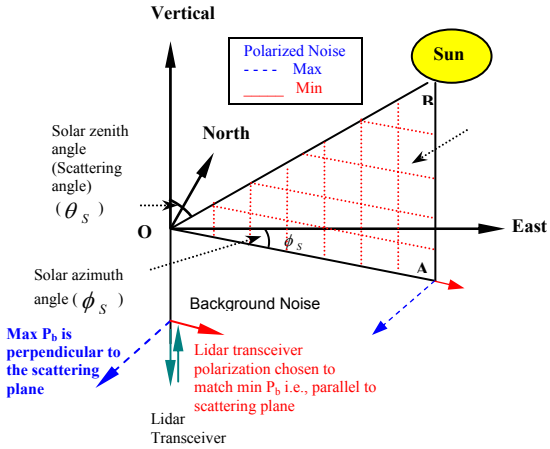

Figure 1: Sky background suppression geometry for a vertical pointing lidar:

The degree of polarization of sky background signal observed by the lidar is largest for solar zenith angles near $\theta_S \approx 90^o$ and smallest at solar noon. The essence of the proposed approach is therefore, at any time, to first determine the parallel component of P_b with a polarizing analyzer on the

receiver, thus minimizing the detected P_b, and then orienting the polarization of the outgoing lidar signal so that the polarization of the received lidar backscatter signal is aligned with the receiver polarizing analyzer, thus maximizing both SNR and attainable lidar ranges.

2. Experimental approach and System geometry

Lidar measurements were performed at the Remote Sensing Laboratory of the City College of New York, (CCNY), with one of several lidars designed to monitor enhanced aerosol events as they traverse the eastern coast of the United States, and forms part of NOAA's Cooperative Remote Sensing Center (CREST) Regional East Atmospheric Lidar Mesonet (REALM) lidar network. The lidar measurements reported here were carried out with a mobile elastic monostatic biaxial backscatter lidar system at the CCNY site (longitude 73.94 W, latitude 40.83 N), at 532 nanometers wavelength. The lidar transmitter uses a Q-switched Nd:YAG Continuum Surelite Laser, coupled to SLD harmonic doubler, producing 300 mj pulses of 7 ns duration at 523 nm, and a 10 Hz repetition rate. The receiver uses a 355.6 mm aperture Schmitt Cassegarian telescope, with a 3910 mm focal length, a Hamamatsu PMT:R11527 photo-multiplier with a 1 nm bandwidth optical filter (532F02-25 Andover). For extended ranges, data is acquired in the photon counting (PC) mode, typically averaging 600 pulses over a one minute interval and using a Licel 40-160 transient recorder with 40 MHz

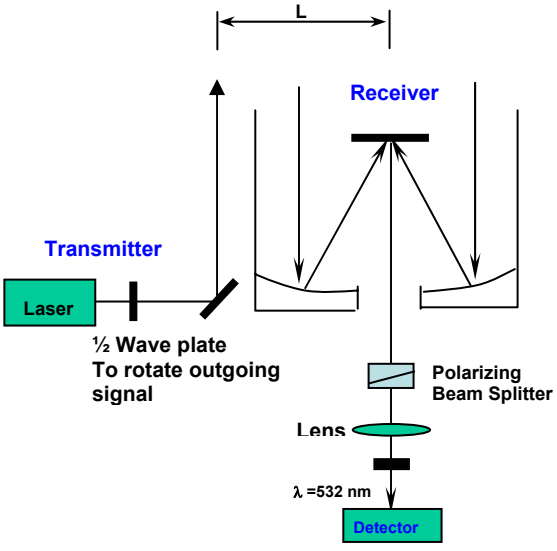

Figure 2: Schematic diagram of polarization experiment set up for elastic biaxial monostatic lidar (mobile lidar) system)

sampling rate for A/D conversion and a 250 MHz photon counting sampling interval. Figure 2 shows the arrangement used to implement the polarization-tracking scheme.

The polarization of light entering the detector is selected by a polarizing beam splitter (with a cross polarized extinction ratio of approximately 10^{-4}) located in front of the collimating lens and narrow band filter. This polarization selector is then rotated to minimize the detected sky background P_b. On the transmission side, a half wave plate at the polarized output of the laser, is then used to rotate the polarization of the outgoing lidar beam so as to align the polarization of the backscattered lidar signal with the receiver polarizing analyzer and hence maximize its throughput (i.e., at the minimum P_b setting). This procedure was repeated for all measurements, with appropriate adjustments being made in receiver polarization analyzer alignment and a corresponding tracking alignment in the transmitted beam polarizations to adjust for different solar angles at different times of the day, thus minimizing the detected P_b and maximizing lidar SNR.

3. Results – Lidar Data

Figure 3 shows an example of experimental results (6:29 PM 07 October 2005) obtained for different polarization alignments. The upper trace

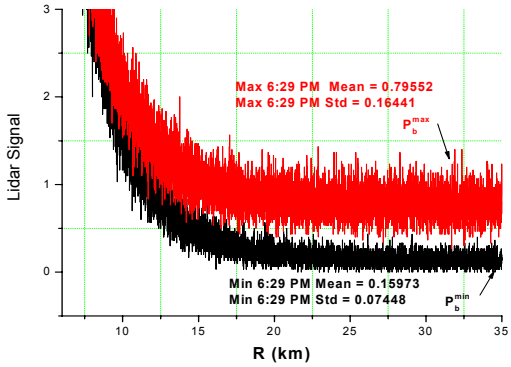

Figure 3: Comparison of max P_b verses min P_b signals

corresponds to the receiver polarization analyzer oriented to minimize P_b and the lidar transmitter polarization oriented to maximize the detected backscattered lidar signal, while the lower trace is the result of orthogonal orientations of both receiver analyzer and lidar polarization, aligned to minimize the sky background component in the return signal. Similar results were obtained at. 3:00 PM and noon on the same day. The relative impact on the sky background signal, $P_{b,}$ of the polarization selection

scheme was found to be largest at 6:29 PM, when the lidar solar angle is large (89°), while at noon it is minimal. For each set of measurements, the detected signal for maximum P_b is much noisier than the detected signal with minimum P_b . The experimental results, which showed that as much as a factor of $\sqrt{10}$ improvement in signal-to-noise ratio over conventional un-polarized schemes can be obtained, were found to be consistent with the shot noise limit applicable to PMT's where the detected noise amplitude (standard deviation) is proportional to the square root of the mean detected background signal. (i.e. $\Delta P \propto \sqrt{\langle P \rangle}$) where P is the detector output, whose mean value is proportional to P_b , confirming that the detector operates in the shot noise limited regime.

To evaluate the potential of the scheme, we compare the detected SNR with and without a polarization selector. When shot noise from background light is large compared to that from the lidar signal backscatter, the SNR improvement can be expressed in terms of an SNR improvement factor (G_{imp}) expressed in terms of maximum and minimum P_b measurements $(P_b^{\max}, P_b^{\min})$ as:

$$G_{imp} = \frac{SNR_{Max}}{SNR_{Unpol}} = \sqrt{\left(\frac{P_b^{\min} + P_b^{\max}}{P_b^{\min}}\right)} = \sqrt{1 + \left(\frac{P_b^{\max}}{P_b^{\min}}\right)} \quad (1)$$

The decreased P_b translates into a SNR improvement, which translates into an equivalent lidar range improvement. Analysis of the experimental results shows that for an SNR=10, the range improvement resulting from polarization selection resulted in an increase in lidar operating range from 9.38 km to 12.5km (a 34% improvement). Alternatively, for a given lidar range, say 9 km, the SNR improvement was 250%. The SNR improvement factor (G_{imp}) was also examined as a function of the local time, and the solar zenith angle. Since the latter retraces itself as the sun passes through solar noon, it would be expected that the improvement factor (G_{imp}) would be symmetric before and after the solar noon and depend solely on the solar zenith angle. This symmetry is generally very well observed on clear dry days.

4.Discussion and analysis

To compare qualitatively the extent of polarization of P_b observed in our experiments with theoretical estimates, we used a single scattering model of the atmosphere accounting for both molecular Rayleigh and aerosol scattering. This is justified by the relatively small optical depths measured by sky radiometry during the experiments. In this limit, P_b is simply proportional to the diffuse transmission, T, of sunlight through the atmosphere. We compared the theoretical model with symmetric data sets which were generally obtained on clear dry days, and good agreement is observed. with the results showing clearly that G_{imp} is significantly affected by the impact of even fairly low levels of aerosols. Small asymmetries were sometimes observed between morning and afternoon readings. These appear to be related to changes in humidity, which can modify the scattering properties and lead to enhanced multiple scattering effects and are supported by the measured variation in PWV[5]. Once the microphysical properties were properly estimated[6], good agreement was found between measurements and theory, using the single scattering model and including measured microphysical properties. We have also examined, in a very preliminary manner, the impact of multiple scattering on the polarization selection technique. While it is intuitive that the maximum noise suppression should occur when the receiver polarization is parallel to the scattering plane in the single scattering regime, it is not so clear that this will hold for multiple scattering. However, it found that even for high optical depth (multiple scattering regime $\tau_{aer} = 0.5$), the maximum noise improvement factor calculated using a full polarized RT code developed at NASA GISS [7] still occurs when the differential azimuth angle is zero.

5. SNR improvement azimuthal dependence

The potential impact of the polarization selection scheme on non-vertically pointing lidars was also examined. Typically, scanning lidars, operating in elastic or Raman backscatter mode, are used to scan for particulates or trace constituents in the troposphere, and are of particular interest to air quality monitoring applications where it is often desired to obtain information on spatial distributions of particulates and trace constituents above an urban area This would include horizontal and near horizontal scans, e.g. along urban canyons etc, where eye safety concerns severely limit acceptable visible lidar pulse energies, so schemes to improve received SNR's are important. Analysis shows that, in contrast to a vertically pointing lidar, where the SNR improvement is greatest when the sun elevation is low, thus restricting the period of improvement to relatively short times in the early morning and late

afternoon, the situation is quite different for a non-vertical scanning lidar. To illustrate, we consider a scanning lidar located at CCNY that is designed to scan the atmosphere above the downtown New York Metropolitan skyline. Since CCNY is approximately 5 km north of the downtown area, the lidar azimuth angle does not need to vary appreciably ($\pm 15^\circ$) and the lidar zenith angle need only vary from $50^\circ \le \theta_{lid} \le 80^\circ$ corresponding to relatively complete coverage through the planetary boundary layer. Under these conditions, we can calculate the resultant scattering angle as a function of the observation time. For all lidars, we find that significant daylight SNR improvement only occurs for scattering angles in the interval $70 < \Theta_{scat} < 110$. As an illustration, we determined the variation in scattering angle for both scanning and vertical configurations for June 21[8], a typically important time of the year for lidar measurements because of the increase in aerosol particulates in summer months. It is found, that for scanning lidars, for a good portion of the day (10:00 AM– 2:00 PM), the scattering angle will lie in the range $70 < \Theta_{scat} < 110$ permitting significant SNR improvement to be obtained by polarization discrimination, in contrast to the situation for a vertically pointing lidar (lidar zenith angle = 0) where these improvements occur for very limited times near sunrise and sunset.

6.Conclusions and Summary

SNR improvements obtained from lidar backscatter measurements, using the polarization selection/tracking scheme to reduce the sky background component, can significantly increase the far range SNR as compared to un-polarized detection. This is equivalent to improvements in effective lidar range of over 30% for a SNR threshold of 10. The improvement is largest for large scattering angles, which for vertical pointing lidars occur near sunrise/sunset. For non-vertical scanning lidars, improvement extends over a significant portion of the midday (10 AM-2 PM), extending the utility of the technique. A theoretical model that simulates the background skylight within the single scattering approximation was developed and showed fairly accurate predictions of the SNR improvement factor. Asymmetric skylight reduction was sometimes observed in experimental results and is explained by the measured increase in PWV and subsequent modification of aerosol optical depth by dehydration from morning to afternoon. Finally, since the polarization axis follows the solar azimuth angle even for high aerosol loading as demonstrated using radiative transfer simulations, it is quite conceivable to automate this procedure simply by using solar position calculators to orient the polarization axes.

Acknowledgements
This work was partially supported under contracts from NOAA # NA17AE1625 and NASA # NCC-1-03009.

References

1. R. M. Schotland, K. Sassen, and R. J. Stone, "Observations by lidar of linear depolarization ratios by hydrometeors," *J. Appl. Meteorol.* **10,** 1011–1017 (1971).
2. Kokkinos, D. S., Ahmed, S. A. "Atmospheric depolarization of lidar backscatter signals" *Lasers '88; Proceedings of the International Conference*, Lake Tahoe, NV, (A90-30956 12-36, McLean, VA, STS Press, 1989), pp. 538-545.
3. N. Roy, G. Roy, L. R. Bissonnette, and J. Simard, "Measurement of the azimuthal dependence of cross-polarized lidar returns and its relation to optical depth," *Appl. Opt.* **43,** 2777-2785 (2004).
4. Yasser Y. Hassebo, Barry M. Gross, Min M. Oo, Fred Moshary, Samir A. Ahmed "Impact on lidar system parameters of polarization selection / tracking scheme to reduce daylight noise" *in Lidar Technologies, Techniques, and Measurements for Atmospheric Remote Sensing,* Upendra N. Singh, ed., Proc. SPIE **5984,** 53-64 (2005).
5. NOAA-CREST webpage: http://earth.engr.ccny.cuny.edu/noaa/wc
6. G. Hanel, "The properties of atmospheric aerosol particles as functions of the relative humidity at thermodynamic equilibrium with the surrounding moist air," *Advances in Geophysics*, H. E. Landsberg and J. Van Mieghem, eds. Academic, New York **19,** 73–188 (1976).
7. J. Chowdhary, B. Cairns, L.D. Travis, "The contribution of the water leaving radiances to multiangle, multispectral polarimetric observations over the open ocean: Bio-optical model results for Case I waters". To appear: Special Issue "Polarization Imaging and Remote Sensing" Appl. Opt.(2006)
8. Solar Calculator Webpage: http://aa.usno.navy.mil/data/docs/AltAz.html